Journal of Molecular Structure 1226 (2021) 129344

Contents lists available at ScienceDirect

Journal of Molecular Structure

journal homepage: www.elsevier.com/locate/molstr

Synthesis and structure of mono and bis {1,3-bis(2-pyridylimino)isoindoline} supported 3d transition metal complexes ☆

G. Reshma [a], Varadha Padmanabhan [a], Arathi R. Varma [a], M.S. Gouri [a], Unnimaya R. Nair [a], P.B. Parvathy [a], Naveen V. Kulkarni [a,*], Dineshchakravarthy Senthurpandi [b]

[a] Department of Chemistry, Amrita Vishwa Vidyapeetham, Amritapuri, Kollam, Kerala, India
[b] Department of Inorganic and Physical Chemistry, Indian Institute of Science, Bangalore, Karnataka, India

ARTICLE INFO

Article history:
Received 28 July 2020
Revised 22 September 2020
Accepted 25 September 2020
Available online 28 September 2020

Keywords:
1,3-bis(2-pyridylimino)isoindolate ligand
3d metal complex
Homoleptic complexes
Heteroleptic complexes

ABSTRACT

Series of homoleptic and heteroleptic 3d transition metal complexes were prepared in analytically pure form and high yield, by reacting appropriate metal precursors with 1,3-bis(2-pyridylimino)isoindolate (BPIH) ligand under suitable reaction conditions. The complexes were characterized by various spectro-analytical techniques, including IR, UV, NMR, ESI Mass and X-ray crystal analysis. A distorted octahedral structure containing two meridionally coordinating BPI ligands was assigned to all the homoleptic complexes. While, for the heteroleptic complexes, a highly distorted square pyramidal geometry, with a planar tridentate BPI ligand coordinating to the metal center along with chloro and aqua ligands was assigned. Considering the unique structural features of the complexes, potential catalytic applications are envisaged.

1. Introduction

Bis(2-pyridylimino)isoindoles (BPIs) are an interesting class of polypyridilamine pincer ligands known for their unique structural features and diverse coordination chemistry. Bis(2-pyridylimino)isoindoles act as a meridionally coordinating pincer ligand system, providing a flexible coordination cavity containing three nitrogen donor sites (NNN) for the metal ion. Depending upon the nature of the metal precursor and the reaction conditions, they can function as an anionic (upon deprotonation) or neutral (no deprotonation) ligands forming either 1:1 or 2:1 (ligand:metal) complexes [1–4].

Enormous number of complexes with varieties of transition metals have been derived from these ligands, which have found versatile applications in various important catalytic processes, including the transfer hydrogenation of ketones and imines [5], dehydrogenation of alcohols and amines [6–9], hydrogenation of alkenes [10–12] and carbon dioxide [13], controlled radical polymerization [14,15], oxidation of hydrocarbons [16–19], dehydrogenative carboxylation of alkanes [20], hydrosilylation [21] and asymmetric cyclopropanation [22] etc. Apart from this, a number of platinum derivatives of BPIs have been used in luminescence applications [23–26]. Conversely, transition metal complexes of this system were also probed as structural models for various enzymes and found to mimic the respective highly selective biological processes, such as, catalase like activity [27,28], superoxide dismutase (SOD) mimic activity [29–32], phenoxazinone synthase mimic activity [33,34], catechol oxidase mimic activity [35,36] etc.

In the current article we report synthesis and characterization of series of homoleptic and heteroleptic first row transition metal complexes derived from a BPI ligand. We believe that, the simple protocols suggested for the synthesis of mono and bis BPI ligated complexes and their structural features established by the thorough spectro-analytical methods in this article would lead to further developments of this system and attract additional applications.

2. Experimental

2.1. Materials and instrumentation

All the chemicals including the ligand precursors, metal salts and solvents were purchased from commercial vendors, Sigma-Aldrich (Merck), Sd-fine, Nice Chemicals, Spectrochem and Thermo Scientific and were used without further purification. The molar conductivity measurement was done by using ELICO–CM-82 conductivity bridge. The IR spectra were recorded using Perkin Elmer FTIR instrument in the range 4000–500 cm^{-1}. The ^1H NMR spectra of the ligand (in $CDCl_3$) and complexes (in DMSO–d6) were recorded on Joel ECZ 500 MHz spectrometer at room temperature.

☆ **Dedicated to Prof. V. K. Revankar on the occasion of his 60th birthday.**

* Corresponding author.
E-mail addresses: dr.naveenvk@gmail.com, naveenvkulkarni@am.amrita.edu (N.V. Kulkarni).

https://doi.org/10.1016/j.molstruc.2020.129344
0022-2860/

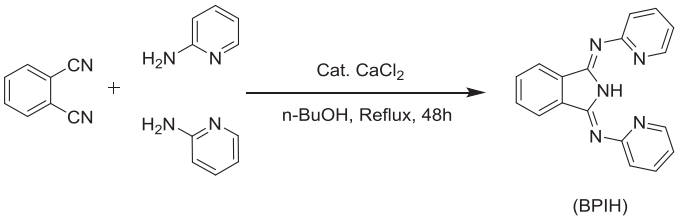

Scheme 1. Preparation of 1,3-bis(2-pyridylimino)isoindolate (BPIH) ligand.

The respective chemical shifts were referenced to solvent residue resonances and are reported relative to Trimethylsilane. The UV-Visible spectra were recorded on a SHIMADZU-1800 UV–VIS spectrophotometer. All the compounds were analyzed for carbon, hydrogen and nitrogen by Thermo Scientific Flash 2000 Organic Elemental Analyzer. Metal and chloride estimation were done by following the established protocols [37]. The mass spectra of the complexes were recorded using Micromass QTOF ESI-MS instrument (model HAB273). The single crystal x-ray study was done using Bruker APEX-II CCD machine.

2.2. Preparation of ligand, 1,3-bis(2-pyridylimino)isoindoline (BPIH)

1,3-bis(2-pyridylimino) isoindoline (BPIH) ligand was prepared by following a reported protocol [1,2,38,39] described below.

Phthalonitrile (10 mmol, 1.28 g) and 2-aminopyridine (20 mmol, 1.88 g) were dissolved in n-butanol (35 ml) in a round bottom flask equipped with a reflux condenser and a catalytic amount of calcium chloride (~ 0.1 mmol, 0.1 g) was added. The reaction mixture was heated to reflux (~180 °C) on a heating mantle for 48 h. After cooling the reaction mixture, a greenish-yellow solid was obtained, which was then filtered and dried under vacuum. The solid obtained was recrystallized using methanol to get the ligand BPIH in a greenish-yellow crystalline form. Yield 70% (Scheme 1) (Note: Comparatively same yield was obtained, when sodium ethoxide (~ 0.1 mmol) was used as a catalyst under similar reaction conditions).

M.P. 180 – 182 °C; IR (ATR, selected, cm^{-1}) 3203 (b), 3062 (w), 1625 (s), 1578 (s), 1552 (s), 1456 (s), 1425 (s), 1374 (m), 1141 (w), 1099 (m); UV–Vis (DMSO) (λ_{max} in nm (log ε in dm^3 mol^{-1} cm^{-1})) 280 (4.19), 297 (4.16), 330 (4.10), 346 (4.11), 370 (4.14), 386 (4.18), 408 (3.95); ^{1}H NMR ($CDCl_3$, 500 MHz, 298 K, ppm) δ 13.97 (1H, br, -NH), 8.61 (2H, m), 8.07 (2H, dd), 7.76 (2H, td), 7.64 (2H, dd), 7.46 (2H, d), 7.11 (2H, m); ^{13}C NMR ($CDCl_3$, 125 MHz, 298 K, ppm) δ = 160.1, 153.1, 148.7, 139.3, 135.5, 132.8, 123.6, 122.9, 121.3; Elemental Analysis for $C_{18}H_{13}N_5$, Calcd (found) C 72.23 (72.32), H 4.38 (4.68), N 23.40 (23.86)%.

2.3. Synthesis of heteroleptic (mono) complexes

Six heteroleptic complexes [BPIH]$MnCl_2$ (C1), [BPI]$FeCl_2$ (C2), [BPI]$Co(H_2O)Cl$ (C3), [BPIH]$NiCl_2$ (C4), [BPIH]$CuCl_2$ (C5) & [BPIH]$ZnCl_2$ (C6) were synthesized by following the method described below.

1 mmol (0.3 g) of 1,3-bis(2-pyridylimino) isoindoline (BPIH), taken in 10 ml of methanol was added dropwise to solution of 1 mmol of corresponding transition metal chloride in 10 ml of methanol in a round bottom flask with continuous stirring. After refluxing for 4 h the mixture was bought to room temperature to get the complex. The solid complex obtained was filtered, washed thoroughly with hot methanol and dried under vacuum.

[BPIH]$MnCl_2$ (C1): BPIH (0.3 g, 1 mmol), $MnCl_2{\cdot}4H_2O$ (0.198 g, 1 mmol). Isolated as a yellow solid. Yield 72%; Molar conductance (Λ_M in DMSO) 6 $ohm^{-1}cm^2$ mol^{-1}; IR (ATR, selected, cm^{-1}) 3204 (b), 3140 (b), 3062 (b), 1654 (m), 1626 (s), 1582 (s), 1553 (s), 1518 (s), 1468 (s), 1456 (s), 1427 (s), 1375 (m), 1099 (m), 1053 (s); UV–Vis (DMSO) (λ_{max} in nm (log ε in dm^3 mol^{-1} cm^{-1}) 275 (4.27), 289 (4.25), 297 (4.24), 319 (4.08), 335 (4.16), 350 (4.18), 370 (4.23), 388 (4.28), 411 (4.05), 455 (2.57); Elemental Analysis for $C_{18}H_{13}C_{l2}N_5Mn$ Calcd. (found) C 50.85 (50.23), H 3.08 (2.86), N 16.47 (16.86), Mn 12.92 (12.82), Cl 16.68 (17.02)%.

[BPI]$FeCl_2$ (C2): BPIH (0.3 g, 1 mmol), $FeCl_3{\cdot}6H_2O$ (0.270 g, 1 mmol). Isolated as a dark brown solid. Yield 65%; Molar conductance (Λ_M in DMSO) 10 $ohm^{-1}cm^2$ mol^{-1}; IR (ATR, selected, cm^{-1}) 3061 (b), 1634 (w), 1604 (m), 1570 (s), 1550 (m), 1523 (w), 1467 (m), 1430 (s), 1386 (m), 1089 (s), 1073 (s); UV–Vis (DMSO) (λ_{max} in nm (log ε in dm^3 mol^{-1} cm^{-1}) 290 (3.96), 298 (3.96), 317 (3.81), 333 (3.73), 350 (3.70), 369 (3.71), 388 (3.71), 412 (3.46), 454 (2.30); Elemental Analysis for $C_{18}H_{12}N_5FeCl_2$ Calcd. (found) C 50.86 (50.51), H 2.85 (2.98), N 16.48 (17.02), Fe 13.14 (13.24), Cl 16.68 (16.42)%.

[BPI]$Co(H_2O)Cl$ (C3): BPIH (0.3 g, 1 mmol). $CoCl_2{\cdot}6H_2O$ (0.237 g, 1 mmol). Isolated as an orange solid. Yield 72%; Molar conductance (Λ_M in DMSO) 7 $ohm^{-1}cm^2$ mol^{-1}; IR (ATR, selected, cm^{-1}) 3300 (b), 1633 (w), 1595 (m), 1566 (s), 1519 (s), 1454 (s), 1361 (w), 1086 (s), 1067 (s); UV–Vis (DMSO) (λ_{max} in nm (log ε in dm^3 mol^{-1} cm^{-1}) 261 (3.74), 291 (3.54), 336 (3.53), 353 (3.43), 394 (3.39), 413 (3.47), 436 (3.48), 490 (3.15); Elemental Analysis for $C_{18}H_{14}N_5OCoCl$, Calcd. (found) C 52.64 (51.92), H 3.44 (3.28), N 17.05 (17.72), Co 14.35 (14.82), Cl 8.63 (8.93)%.

[BPIH]$NiCl_2$ (C4): BPIH (0.3 g, 1 mmol), $NiCl_2{\cdot}6H_2O$ (0.237 g, 1 mmol). Isolated as a green solid. Yield 68%; Molar conductance (Λ_M in DMSO) 4 $ohm^{-1}cm^2$ mol^{-1}; IR (ATR, selected, cm^{-1}) 3325 (b), 3078 (b), 1659 (w), 1636 (m), 1625 (m), 1612 (w), 1599 (w), 1564 (m), 1552 (m), 1529 (s), 1479 (s), 1463 (s), 1429 (s), 1378 (m), 1109 (s), 1084 (m); UV–Vis (DMSO) (λ_{max} in nm (log ε in dm^3 mol^{-1} cm^{-1}) 278 (4.22), 296 (4.20), 336 (4.23), 350 (4.20), 370 (4.16), 390 (4.21), 412 (4.01), 436 (4.01), 464 (3.83); Elemental Analysis for $C_{18}H_{13}N_5NiCl_2$ Calcd. (found) C 50.40 (50.34), H 3.06 (2.98), N 16.33 (16.89), Ni 13.68 (13.12), Cl 16.53 (16.28)%; ESI mass (*m/z*), 356.04 ([BPI]Ni^+).

[BPIH]$CuCl_2$ (C5): BPIH (0.3 g, 1 mmol), $CuCl_2{\cdot}2H_2O$ (0.17 g, 1 mmol). Isolated as a green solid. Yield 70%; Molar conductance (Λ_M in DMSO) 6 $ohm^{-1}cm^2$ mol^{-1}; IR (ATR, selected, cm^{-1}) 3329 (b), 1663 (w), 1632 (m), 1598 (w), 1580 (s), 1532 (s), 1485 (m), 1466 (s), 1437 (m), 1381 (w), 1113 (m), 1101 (m); UV–Vis (DMSO) (λ_{max} in nm (log ε in dm^3 mol^{-1} cm^{-1}) 276 (3.98), 298 (3.91), 319 (3.80), 333 (3.89), 351 (3.88), 371 (3.90), 389 (3.92), 413 (3.69), 475 (3.26); Elemental Analysis for $C_{18}H_{13}N_5CuCl_2$ Calcd. (found) C 49.84 (50.23), H 3.02 (3.08), N 16.15 (16.68), Cu 14.65 (14.28), Cl 16.34 (16.30)% ESI mass (m/z), 361.04 ([BPI]Cu^+).

[BPIH]$ZnCl_2$ (C6): BPIH (0.3 g, 1 mmol), $ZnCl_2$ (0.136 g, 1 mmol). Isolated as a yellow solid. Yield 72%; Molar conductance (Λ_M in DMSO) 4 $ohm^{-1}cm^2$ mol^{-1}; IR (ATR, selected, cm^{-1}) 3292 (b), 3143 (b), 3078 (b), 1656 (m), 1628 (s), 1614 (m), 1592 (m), 1556 (m), 1520 (s), 1487 (s) 1431 (m), 1375 (w), 1101 (m), 1065 (m), 1056 (m); UV–Vis (DMSO) (λ_{max} in nm (log ε in dm^3 mol^{-1} cm^{-1}) 280 (4.22), 296 (4.20), 319 (4.05), 333 (4.10), 350 (4.11), 370 (4.16), 389 (4.20), 418 (3.97); ^{1}H NMR (DMSO–d_6, 500 MHz, 298 K, ppm) δ 13.92 (1H, br, -NH), 8.66 (2H, br), 8.03 (2H, br), 7.85 (2H, br), 7.71 (2H, br), 7.43 (2H, br), 7.21 (2H, br); Elemental Analysis for $C_{18}H_{13}N_5ZnCl_2$ Elemental Analysis Calcd. (found) C 49.63 (49.32), H 3.01 (2.82), N 16.08 (15.62), Zn 15.01 (15.36), Cl 16.28 (16.16)%.

2.4. Synthesis of homoleptic (bis) complexes

Six homoleptic complexes, $[BPI]_2Mn$ (C7), $[\{BPI\}_2Fe]Cl$ (C8), $[BPI]_2Co$ (C9), $[BPI]_2Ni$ (C10), $[BPI]_2Cu$ (C11) & $[BPI]_2$ Zn (C12) were synthesized by following the method described below.

1 mmol (0.3 g) of ligand, BPIH, in 10 ml of methanol was added dropwise to solution of 0.5 mmol of respective metal precursor in

10 ml of methanol in a round bottom flask with continuous stirring. Few drops of 25% ammonia (or 0.1 N potassium hydroxide) solution were added to the reaction mixture. The mixture was then refluxed on a water bath overnight and cooled to room temperature. The solid obtained was filtered and dried under vacuum.

$[BPI]_2Mn$ (C7): BPIH (0.3 g, 1 mmol) and $Mn(NO_3)_2{\cdot}4H_2O$ (0.126 g, 0.5 mmol), following the protocol described above. Isolated as a brownish yellow solid. Yield 77%; Molar conductance (Λ_M in $ohm^{-1}cm^2\ mol^{-1}$) 8; IR (ATR, selected, cm^{-1}) 3050 (b), 1631 (w), 1594 (w), 1569 (s), 1549 (w), 1525 (s), 1461 (s), 1425 (m), 1366 (w), 1089 (s), 1066 (s); UV–Vis (DMSO) (λ_{max} in nm (log ε in $dm^3\ mol^{-1}\ cm^{-1}$) 286 (3.90), 313 (3.98), 335 (3.90), 371 (3.82), 393 (4.00), 418 (4.08), 448 (3.81); Elemental Analysis for $C_{36}H_{24}N_{10}Mn$, Calcd. (found) C 66.36 (65.92), H 3.71 (3.81), N 21.50 (22.01), Mn 8.43 (8.13)%.

$[\{BPI\}_2Fe]Cl$ (C8): BPIH (0.3 g, 1 mmol) and $FeCl_3{\cdot}6H_2O$ (0.135 g, 0.5 mmol), following the protocol described above. Isolated as a dark brown solid. Yield 72%; Molar conductance (Λ_M in DMSO) 38 $ohm^{-1}cm^2\ mol^{-1}$; IR (ATR, selected, cm^{-1}) 3062 (b), 1634 (w), 1567 (w), 1523 (s), 1455 (s), 1425 (s), 1364 (w), 1095 (s), 1073 (s); UV–Vis (DMSO) (λ_{max} in nm (log ε in $dm^3\ mol^{-1}\ cm^{-1}$) 257 (4.01), 265 (3.83), 298 (3.86), 318 (3.77), 332 (3.69), 349 (3.67), 368 (3.61), 388 (3.60), 412 (3.35), 454 (2.27); Elemental Analysis for $C_{36}H_{24}N_{10}FeCl$ Calcd. (found) C 62.85 (63.48), H 3.52 (3.82), N 20.36 (21.01), Fe 8.12 (8.20), Cl 5.15 (4.85)%; ESI mass (m/z), 652.16 ($[BPI]_2Fe^+$).

$[BPI]_2Co$ (C9): BPIH (0.3 g, 1 mmol) and $Co(NO_3)_2{\cdot}6H_2O$ (0.146 g, 0.5 mmol), following the protocol described above. Isolated as an orange red solid (A saturated solution of the pure compound in MeOH:DCM (1:1) was stored at 2–4 °C for two days to obtain the crystals suitable for X-ray analysis). Yield 76%; Molar conductance (Λ_M in DMSO) 7 $ohm^{-1}cm^2\ mol^{-1}$; IR (ATR, selected, cm^{-1}) 3196 (b), 1633 (w), 1594 (w), 1565 (s), 1552 (w), 1519 (s), 1454 (s), 1388 (w), 1086 (s), 1067 (s); UV–Vis (DMSO) (λ_{max} in nm (log ε in $dm^3\ mol^{-1}\ cm^{-1}$) 288 (3.93), 297 (3.93), 320 (3.89), 334 (3.89), 350 (3.79), 369 (3.70), 391 (3.86), 413 (3.94), 437 (3.85), 502 (2.46); Elemental Analysis for $C_{36}H_{24}N_{10}Co$ Calcd. (found) C 65.96 (65.43), H, 3.69 (3.82), N 21.37 (21.84), Co 8.99 (9.25)%;

$[BPI]_2Ni$ (C10): BPIH (0.3 g, 1 mmol) and $Ni(NO_3)_2{\cdot}6H_2O$ (0.145 g, 0.5 mmol), following the protocol described above. Isolated as a brown solid. Yield 72%; Molar conductance (Λ_M in DMSO) 6 $ohm^{-1}cm^2\ mol^{-1}$; IR (ATR, selected, cm^{-1}) 3058 (b), 1636 (w), 1567 (s), 1552 (w), 1522 (s), 1455 (s), 1384 (w), 1087 (s), 1071 (s); UV–Vis (DMSO) (λ_{max} in nm (log ε in $dm^3\ mol^{-1}\ cm^{-1}$) 258 (3.95), 296 (3.86), 325 (3.92), 340 (3.87), 360 (3.65), 409 (3.82), 436 (4.01), 464 (4.00), 514 (2.32); Elemental Analysis for $C_{36}H_{24}N_{10}Ni$ Calcd. (found) C 65.98 (66.23), H 3.69 (4.02), N 21.37 (21.68), Ni, 8.96 (9.20)%; ESI mass (m/z), 656.16 ($[BPI]_2NiH^+$).

$[BPI]_2Cu$ (C11): BPIH (0.3 g, 1 mmol) and $Cu(OAc)_2.H_2O$ (0.099 g, 0.5 mmol), following the protocol described above. Isolated as a green solid. Yield 70%; Molar conductance (Λ_M in DMSO) 7 $ohm^{-1}cm^2\ mol^{-1}$; IR (ATR, selected, cm^{-1}) 3046 (b), 1632 (w), 1580 (s), 1552 (w), 1533 (s), 1465 (s), 1433 (s), 1377 (m), 1088 (s), 1068 (s); UV–Vis (DMSO) (λ_{max} in nm (log ε in $dm^3\ mol^{-1}\ cm^{-1}$) 278 (4.04), 315 (4.03), 340 (4.01), 357 (3.86), 404 (3.88), 428 (4.05), 456 (3.96); Elemental Analysis for $C_{36}H_{24}N_{10}Cu$ Calcd. (found) C 65.49 (65.12); H 3.66 (3.82), N 21.22 (21.62), Cu 9.63 (10.02)%; ESI mass (m/z), 660.16 ($[BPI]_2CuH^+$).

$[BPI]_2$ Zn (C12): BPIH (0.3 g, 1 mmol) and $Zn(OAc)_2{\cdot}2H_2O$ (0.109 g, 0.5 mmol), following the protocol described above. Isolated as a yellow solid. Yield 76%; Molar conductance (Λ_M in DMSO) 6 $ohm^{-1}cm^2\ mol^{-1}$; IR (ATR, selected, cm^{-1}) 3044 (b), 1631(m), 1599 (w), 1569 (m), 1551 (s), 1533 (s), 1465 (s), 1450 (w), 1432 (m), 1367 (m), 1095 (s), 1074 (s); UV–Vis (DMSO) (λ_{max} in nm (log ε in $dm^3\ mol^{-1}\ cm^{-1}$) 288 (4.20), 311 (4.17), 336 (4.18), 370 (4.08), 392 (4.20), 417 (4.24), 446 (4.07); ^1H NMR (DMSO–d_6, 500 MHz, 298 K, ppm) δ 8.58 (2H, br), 7.92–7.87 (4H, m), 7.60 (2H, d), 7.43 (2H, d), 7.20 (2H, t); Elemental Analysis for $C_{36}H_{24}N_{10}Zn$ Calcd. (found) C 65.31 (65.68), H 3.65 (3.42), N 21.16 (21.82), Zn, 9.88 (9.62)%; ESI mass (m/z), 661.16 ($[BPI]_2ZnH^+$).

2.5. X-ray crystal analysis

A good quality single crystal of the size 0.085 × 0.117 × 0.265 mm of the homoleptic cobalt complex (C9) was chosen under the polarizing microscope for diffraction studies. Crystal was separated using brush and mounted on a nylon loop with the help of paratone oil. Intensity data were collected on Bruker APEX-II CCD machine at 296(2)K, room temperature. All data were integrated with SAINT and a multi-scan absorption correction using SADABS-2012/1 was applied. The structure was solved by direct methods using SHELXS-97 [40] and refined by full-matrix least-squares methods against F^2 by SHELXL-2018/1 [40]. All non-hydrogen atoms were refined with anisotropic displacement parameters. The hydrogen atoms were refined isotropically on calculated positions using a riding model (HFIX 43) with their U_{iso}values constrained to 1.2 times the U_{eq} of their pivot atoms. Main structural entity and the solvent molecule, dichloromethane, both sit on the special position 2-fold axis. Hydrogen atom(H200) bonded to the carbon atom(C200) of the solvent molecule have been found in the difference Fourier and its positions was refined freely, whereas its U_{iso}value constrained to 1.2 times of the parent atom. Graphics and publication materials were prepared with the help of Ortep-III for windows [41] and WinGX suite [41] programs respectively.

3. Result and discussion

3.1. Synthesis of ligand

1,3-bis(2-pyridylimino) isoindoline (BPIH) ligand was prepared by reacting pthalonitrile and 2-aminopyridine (1:2) in n-butanol, in the presence of catalytic amount of calcium chloride or sodium ethoxide (Scheme 1) [1,2,38,39]. Structure and analytical purity of the ligand was confirmed by the various spectro-analytical techniques, as described below.

3.2. Synthesis of complexes

Six heteroleptic transition metal complexes $[BPIH]MnCl_2$ (C1), $[BPI]FeCl_2$ (C2), $[BPI]Co(H_2O)Cl$ (C3), $[BPIH]NiCl_2$ (C4), $[BPIH]CuCl_2$ (C5), $[BPIH]ZnCl_2$ (C6) and six homoleptic transition metal complexes, $[BPI]_2Mn$ (C7), $[\{BPI\}_2Fe]Cl$ (C8), $[BPI]_2Co$ (C9), $[BPI]_2Ni$ (C10), $[BPI]_2Cu$ (C11) & $[BPI]_2$ Zn (C12) were prepared by reacting BPIH ligand with the corresponding metal precursor, in 1:1 and 2:1 ratio respectively, in methanol under suitable reaction conditions. Structure and analytical purity of the complexes was confirmed by the various spectro-analytical techniques (*vide infra*) and compared with the related compounds reported in literature. The proposed structures of the complexes are depicted in Scheme 2.

3.3. Structural elucidation

The ligand BPIH and all the twelve 3d transition metal complexes were analyzed by various spectro-analytical methods, including, molar conductivity measurements, IR, UV, NMR and mass spectral analysis as well as elemental analysis and their structure and analytical purity was confirmed (*vide infra*).

3.3.1. Molar conductivity measurements

The molar conductance of all the homoleptic and heteroleptic complexes (C1-C12) was measured at room temperature in

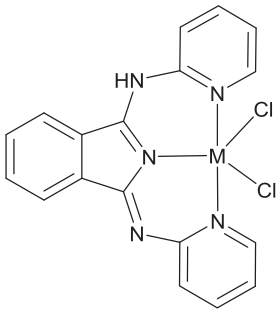

C1: M = Mn
C4: M = Ni
C5: M = Cu
C6: M = Zn

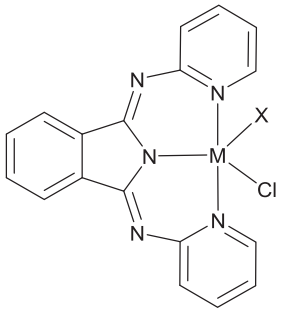

C2: M = Fe, X = Cl
C3: M = Co, X = H_2O

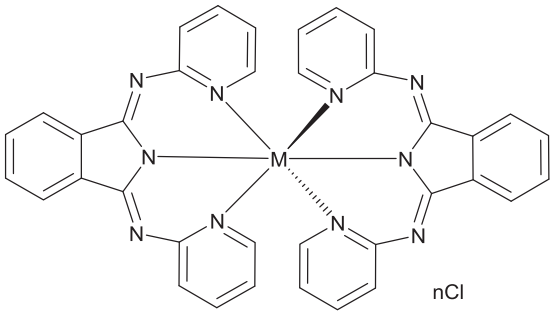

C7 M = Mn(II), n = 0
C8 M = Fe(III), n = 1
C9 M = Co(II), n = 0
C10 M = Ni(II), n = 0
C11 M = Cu(II), n = 0
C12 M = Zn(II), n = 0

Scheme 2. Projected structures of the complexes C1-C12.

DMSO solution with 10^{-3} mol/dm^3 concentration. The values of Λ_M for all the complexes were found to be below 10 ohm^{-1}cm^2 mol^{-1} indicating a non-electrolytic nature of the complexes, except for the iron complex C8, which showed higher conductivity (Λ_M = 38 ohm^{-1}cm^2 mol^{-1}, 1:1 electrolyte) indicating its ionic nature [42,43,44].

3.3.2. Infrared spectroscopy studies

Infrared spectrum of the ligand BPIH, shows broad 'V' shaped absorption around 3300 cm^{-1} which is typical for –NH stretching (from isoindoline ring) and the bands around 3000 cm^{-1} are attributed to the aromatic –CH stretching. Several absorptions observed in the range 1650–1350 cm^{-1} which are characteristic for this ligand molecule are attributed to the coupled modes involving the imines and the 2-pyridine groups. In the complexes, C2, C3 & C7–C12, disappearance of -NH band indicates the coordination of the indole nitrogen upon deprotonation. A significant change in the absorption pattern in the region 1650–1350 cm^{-1} was observed in all these complexes, due to the deprotonation and the subsequent coordination. Further, typical weak absorptions observed around 1630, 1590 & 1450 cm^{-1} and strong absorptions observed around 1530 1465, 1095 & 1074 cm^{-1} confirm the presence of a deprotonated isoindoline ligand. In the case of complexes C1, C4, C5 &C6, strong to medium intensity absorptions observed around 1655, 1630 & 1100 cm^{-1}, and a weak absorption observed around 3300 cm^{-1} suggest the presence of a neutral, non-deprotonated isoindoline ligand in these complexes. Alongside the lower frequency shifts, decrease in the intensity observed for the characteristic pyridyl skeletal bands in all complexes due to the participation of pyridyl ring nitrogen in the metal coordination. A broad absorption band observed for the complex C3 around 3300 cm^{-1} is attributed to the OH stretching of the coordinated water molecule. [45–47].

3.3.3. NMR studies

The ^{1}H NMR of the ligand BPIH (in $CDCl_3$) exhibited seven well separated peaks, with the chemical shift and integration values as well as the multiplicity of all the peaks fitting well with the expected structure of the ligand. The aromatic protons of the isoindoline moiety appear at lower field due to the de-shielding effect of the imino (C=*N*-) functionality. The isoindoline -NH was observed at 14 ppm, indicating its highly acidic nature [38]. In the corresponding ^{13}C NMR spectrum, total nine peaks were observed owing to nine types of the carbons present in the molecule. The peak at 160.1 ppm is assigned to the α carbon of pyridine rings, and the peak at 153.1 ppm is ascribed to exo-C=N carbon, all the other peaks observed in the range 120−150 ppm are attributed to the aromatic ring carbons.

^{1}H NMR spectrum of the heteroleptic zinc complex C6, measured in DMSO–d6, displayed 7 peaks. The broad peak observed at δ13.92 ppm is attributed to the -NH proton indicating the neutral coordination mode of the ligand. All the other six peaks observed in the aromatic region are assigned to isoindoline and pyridine ring protons. In the case of homoleptic zinc complex, C12, absence of the -NH peak indicates the coordination of isoindoline nitrogen upon deprotonation. However no significant change in the chemical shift values of the aromatic protons of isoindoline and pyridine ring was observed. All the aromatic peaks in both the complexes were found to be relatively broad and their symmetric pattern suggest the typical planar NNN coordination mode of the ligand [2,48].

3.3.4. UV-Visible spectroscopy studies

UV–visible spectra of ligand BPIH and its mono (C1-C6) and bis (C7-C12) complexes were recorded in DMSO (10^{-4} M) in the range 270–900 nm. In the electronic spectrum of the ligand, peaks observed in the range 270–300 nm are assigned to the $\pi \rightarrow \pi^*$ transitions associated with the aromatic groups [45]. Multiple absorptions observed at higher wavelength range, 300–415 nm are assigned to intra-ligand n $\rightarrow \pi^*$ transitions mainly associated with C=N groups of pyridine ring as well as exo-C=N group [1,45]. In the complexes C2, C3 & C7-C12, the shapes and intensities of the intra ligand $\pi \rightarrow \pi^*$ and n $\rightarrow \pi^*$ transitions, observed in the range 270–300 and 300–415 nm respectively, experience a significant change suggesting the presence of deprotonated form of the ligand in these complexes [2,29,48]. While in the case of complexes C1 & C4-C6 these peaks remain mostly unaltered indicating the neutral coordination mode of the ligand. Slight changes observed in the absorption values are however attributed to the change in the electronic environment of the ligand upon coordination to the metal. The LMCT transitions are observed in the range 430 – 475 nm [28,45,48]. The cobalt complex C9 and nickel complex C10 exhibited weak absorption peaks around 500 nm, attributed to the d-d transitions [2,16,30].

3.3.5. Elemental analysis and mass spectrometric studies

Results from the C, H, N analysis and metal and chloride estimations are in fine agreement with the empirical formulae of the prepared compounds (Scheme 2) and hence confirm their analytical purity.

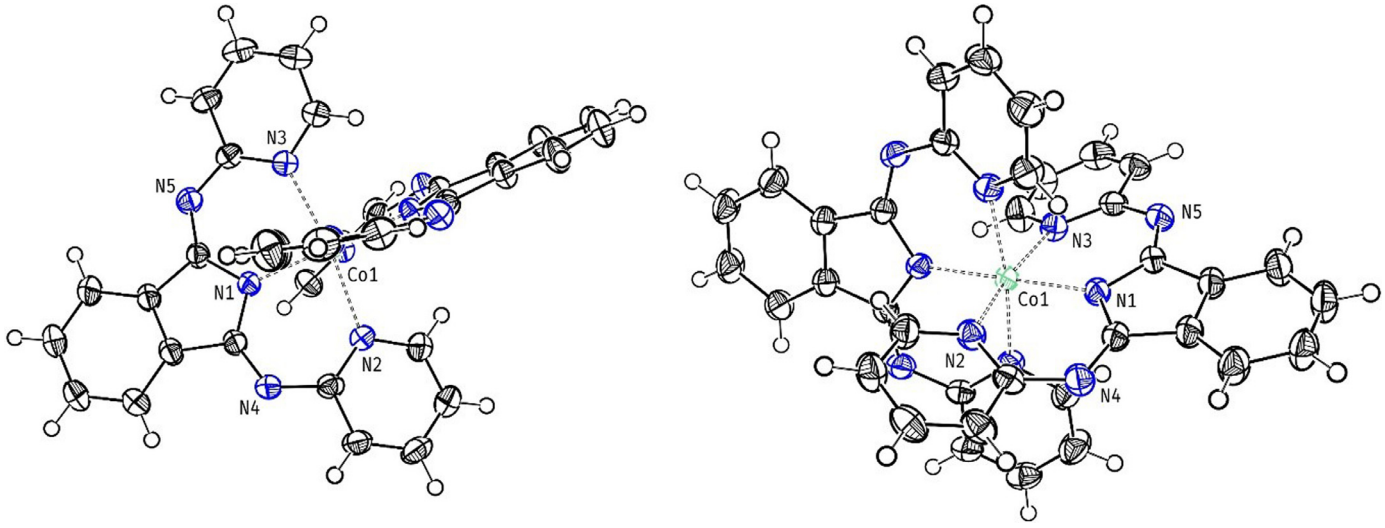

Fig. 1. Molecular structure of the complex C9 (views from two different angles) ORTEP diagram - thermal ellipsoids set at 50% probability (solvent molecule, DCM was removed for the clarity). Selected bond lengths and angles: Co(1)-N(1) = 2.007(2), Co(1)-N(1)#2 = 2.007(2), Co(1)-N(2) = 2.149(2), Co(1)-N(2)#2 = 2.149(2), Co(1)-N(3)#2 = 2.168(2), Co(1)-N(3) = 2.168(2) Å. N(2)#2-Co(1)-N(3)#2 = 171.59(9), N(1)-Co(1)-N(3) = 85.54(9), N(1)#2-Co(1)-N(3) = 94.02(9), N(2)-Co(1)-N(3) = 171.59(9)°.

ESI mass spectra of the heteroleptic nickel (C4) and copper (C5) complexes exhibited higher intensity peaks at m/z 356 and 361, which are attributed to the molecular ions, $[BPI]Ni^{+}$ (M) and $[BPI]Cu^{+}$ (M) respectively (due to loss of two chlorides and ligand deprotonation). In the case of homoleptic iron (C8), nickel (C10) and copper (C11) complexes, higher intensity peaks observed at m/z 652, 655 and 660 are ascribed to the molecular ions, $[BPI]_2Fe^{+}$(M), $[BPI]_2NiH^{+}$ $(M + 1)$ and $[BPI]_2CuH^{+}$ $(M + 1)$ respectively. These mass peaks support the proposed stoichiometry and structures of the complexes. In all the three mass spectra, base peak is observed at m/z 300, which is consistent with the mass of ligand molecular ion, $[BPIH]H^{+}(M + 1)$ [49].

3.3.6. X-ray diffraction studies

The molecular structure of the cobalt complex C9 is shown in Fig. 1 along with the list of some selected bond lengths and bond angles. The complex is comprised of two tridentate anionic BPI ligands meridionally bound to the cobalt(II) center, *via* isoindoline and two pyridine nitrogen atoms. The two ligand planes essentially remain perpendicular to each other. The coordination geometry around the cobalt(II) ion is found to be 'distorted octahedral', with all the donor nitrogen atoms of the two ligand units occupying the six tips. In the complex, the Co–N (isoindoline) bond distance (2.007 A°) is found to be significantly shorter than the two Co–N (pyridine) bond lengths (2.149 & 2.168 Å) indicating the stronger coordination of the deprotonated isoindoline nitrogen. The difference in the Co–N bond distances of two pyridine sidearms is attributed to the steric constraints. All three Co–N bond lengths of this complex are found to be comparable to the analogues cobalt complex having a methyl substituted BPI ligand [16], and are significantly longer than the bonds reported for the Co(III) complex containing the same BPI ligand [50]. The N(pyridine)–Co–N(pyridine) bond angles are found to be 171 °C, indicating the slight distortion in the planarity of the ligand around the cobalt (II) center.

4. Conclusion

Six of each heteroleptic and homoleptic 3d transition metal complexes of a bis(2-pyridylimino)isoindoline(BPIH) ligand were obtained in analytically pure form in high yields. All the complexes were characterized by various spectro-analytical tools. From the data, a distorted octahedral structure, containing two meridionally coordinating BPI ligands was assigned to the homoleptic complexes (C7-C12). Which was further confirmed by the X-ray studies in the case of the cobalt complex C9. Heteroleptic complexes (C1-C6) were proposed to have a highly distorted square pyramidal geometry, with a planar tridentate BPI ligand, chloro and aqua ligands coordinating to the metal center. The homoleptic iron complex C8 was found to be cationic in nature. Interestingly, the heteroleptic manganese (C1) and cobalt (C3) complexes were found to be active catalysts in the Guerbet upgradation of ethanol. We are currently working on the methodology to improve the conversion and selectivity of the reaction.

Supporting information

Representative infrared, electronic, NMR and mass spectra of the compounds and details of the single crystal analysis of the compound **C9** are provided in Supporting Information (the structural data of **C9** is deposited with the Cambridge Crystallographic Data Centre - CIF file CSD no. 2006565; http://www.ccdc.cam.ac.uk/).

Declaration of Competing Interest

Here with we declare that there are no known competing financial interests or personal relationships that could influence the work reported in this paper.

CRediT authorship contribution statement

G. Reshma: Formal analysis, Investigation, Data curation, Writing - original draft. **Varadha Padmanabhan:** Formal analysis, Investigation. **Arathi R. Varma:** Investigation, Validation. **M.S. Gouri:** Investigation, Validation. **Unnimaya R. Nair:** Validation. **P.B. Parvathy:** Validation. **Naveen V. Kulkarni:** Conceptualization, Formal analysis, Investigation, Data curation, Funding acquisition, Methodology, Project administration, Resources, Supervision, Validation, Visualization, Writing - original draft, Writing - review & editing. **Dineshchakravarthy Senthurpandi:** Investigation, Data curation, Writing - original draft.

Acknowledgements

We would like to thank, Dr. Kamalesh Kumar (Banaras Hindu University, Varanasi) and Dr. Animesh Das (Indian Institute of Technology Guwahati) for their help in the spectro-analytical analysis of the compounds.

Supplementary materials

Supplementary material associated with this article can be found, in the online version, at doi:10.1016/j.molstruc.2020.129344.

References

[1] W.O. Siegl, J. Org. Chem. 42 (11) (1977) 1872–1878.
[2] R.R. Gagne, W.A. Marritt, D.N. Marks, W.O. Siegl, Inorg. Chem. 20 (1981) 3260–3267.
[3] D.C. Sauer, R.L. Melen, M. Kruck, L.H. Gade, Eur. J. Inorg. Chem. 28 (2014) 4715–4725.
[4] R. Csonka, G. Speiera, J. Kaizer, RSC Adv. 5 (2015) 18401–18419.
[5] L. Müller, T. Bleith, T. Roth, H. Wadepohl, L.H. Gade, Organometallics 34 (2015) 2326–2342.
[6] K.-N.T. Tseng, J.W. Kampf, N.K. Szymczak, Organometallics 32 (7) (2013) 2046–2049.
[7] K.-N.T. Tseng, A.M. Rizzi, N.K. Szymczak, J. Am. Chem. Soc. 135 (44) (2013) 16352–16355.
[8] K-N.T. Tseng, J.W. Kampf, N.K. Szymczak, ACS Catal. 5 (2015) 5468–5485.
[9] K.-N.T. Tseng, S. Lin, J.W. Kampf, N.K. Szymczak, Chem. Commun. 52 (2016) 2901–2904.
[10] B. Siggelkow, M.B. Meder, C.H. Galka, L.H. Gade, Eur. J. Inorg. Chem. 17 (2004) 3424–3435.
[11] M.B. Meder, I. Haller, L.H. Gade, Dalton Trans. 34 (2005) 1403–1415.
[12] B.A. Siggelkow, L.H. Gade, Z. Anorg, Allg. Chem. 631 (2005) 2575–2584.
[13] N. Planas, T. Ono, L. Vaquer, P. Miro, J. Benet-Buchholz, L. Gagliardi, C.J. Cramer, A. Llobet, Phys. Chem. Chem. Phys. 13 (43) (2011) 19480–19484.
[14] J.A. Camerano, A.S. Rodrigues, F. Rominger, H. Wadepohl, L.H. Gade, J. Organomet. Chem. 696 (7) (2011) 1425–1431.
[15] B.K. Langlotz, J.L. Fillol, J.H. Gross, H. Wadepohl, L.H. Gade, Chem. Eur. J. 14 (2008) 10267–10279.
[16] C.A. Tolman, J.D. Druliner, P.J. Krusic, M.J. Nappa, W.C. Seidel, I.D. Williams, S.D. Ittel, J. Mol. Cat. 48 (1988) 129–148.
[17] L. Saussine, E. Brazi, P.A. Robine, H. Mimoun, J. Fischer, R. Weiss, J. Am. Chem. Soc. 107 (1985) 3534–3540.
[18] E.T. Farinas, C.V. Nguyen, P.K. Mascharak, Inorg. Chim. Acta 263 (1997) 17–21.
[19] F.A. Chavez, P.K. Mascharak, Acc. Chem. Res. 33 (2000) 539–545.
[20] B.L. Tran, M. Driess, J.F. Hartwig, J. Am. Chem. Soc. 136 (2014) 17292–17301.
[21] B.K. Langlotz, H. Wadepohl, L.H. Gade, Angew. Chem. Int. Ed. 47 (2008) 4670–4674.
[22] D.C. Sauer, H. Wadepohl, L.H. Gade, Inorg. Chem. 51 (2012) 12948–12958.
[23] H.-.M. Wen, Y.H. Wu, Y. Fan, L.-Y. Zhang, C.-N. Chen, Z.-N. Chen, Inorg. Chem. 49 (2010) 2210–2221.
[24] H.-M. Wen, Y.-H. Wu, L.-J. Xu, L.-Y. Zhang, C.-N. Chen, Z.- N. Chen, Dalton Trans. 40 (2011) 6929–6938.
[25] K. Hanson, L. Roskop, P.I. Djurovich, F. Zahariev, M.S. Gordon, M.E. Thompson, J. Am. Chem. Soc. 132 (2010) 16247–16255.
[26] K. Hanson, L. Roskop, N. Patel, L. Griffe, P.I. Djurovich, M.S. Gordon, M.E. Thompson, Dalton Trans. 41 (2012) 8648–8659.
[27] J. Kaizer, B. Kriplia, G. Speier, L. Párkányi, Polyhedron 28 (2009) 933–936.
[28] J. Kaizer, G. Barath, G. Speier, M. Reglier, M. Giorgi, Inorg. Chem. Comm. 10 (2007) 292–294.
[29] J.S. Pap, B. Kripli, V. Banyai, M. Giorgi, L. Korez, T. Gajda, D. Arus, J. Kaizer, G. Speier, Inorg. Chem. Acta 376 (2011) 158–169.
[30] J.S. Pap, B. Kripli, T. Váradi, M. Giorgi, J. Kaizer, G. Speier, J. Inorg. Biochem. 105 (2011) 911–918.
[31] B. Kripli, G. Baráth, É. Balogh-Hergovich, M. Giorgi, A.J. Simaan, L. Párkányi, J.S. Pap, J. Kaizer, G. Speier, Inorg. Chem. Commun. 14 (2011) 205–209.
[32] J.S. Pap, B. Kripli, M. Giorgi, J. Kaizer, G. Speier, Trans. Met. Chem 36 (2011) 481–489.
[33] M. Szávuly, R. Csonka, G. Speier, R. Barabás, M. Giorgi, J. Kaizer, J. Mol. Catal. A Chem. 392 (2014) 120–126.
[34] J. Kaizer, G. Barath, R. Csonka, G. Speier, L. Korecz, A. Rockenbauer, L. Párkányi, J. Inorg. Biochem. 102 (2008) 773–780.
[35] Á. Kupán, J. Kaizer, G. Speier, M. Giorgi, M. Réglier, F. Pollreisz, J. Inorg. Biochem. 103 (2009) 389–395.
[36] T. Csay, B. Kripli, M. Giorgi, J. Kaizer, G. Speier, Inorg. Chem. Commun. 13 (2010) 227–230.
[37] A.I. Vogel, A Text book of Quantitative Inorganic Analysis, 3rd Edn, Longmans Green and Co. Ltd., London, 1961.
[38] W. Schilf, J. Mol. Struct. 691 (2004) 141–148.
[39] M. Wekes, D. Jagany, Dalton Trans. 43 (2014) 2549–2558.
[40] G.M. Sheldrick, Acta Crystallogr., Sect. A 64 (2008) 112–122.
[41] L.J. Farrugia, J. Appl. Cryst. 30 (1997) 565.
[42] N.V. Kulkarni, A. Kamath, S. Budagumpi, V.K. Revankar, J. Mol. Struct. 1006 (2011) 580–588.
[43] N.V. Kulkarni, V.K. Revankar, J. Coord. Chem. 64 (4) (2011) 725–741.
[44] W.J. Geary, Coord. Chem. Rev. 7 (1971) 81–122.
[45] E. Balogh-Hergovich, G. Speier, M. Reglier, M. Giorgi, E. Kuzmann, A. Vertes, Inorg. Chem. Comm. 8 (2005) 457–459.
[46] D.M. Baird, W.P. Maehlmann, R.D. Bereman, P. Singh, J. Coord. Chem. 42 (1997) 107–126.
[47] T.Csay Kaizer, P. Kovari, G. Speier, L. Parkanyi, J. Mol. Cat. A 280 (2008) 203–209.
[48] M.A. Robinson, S.I. Trotz, T.J. Hurley, Inorg. Chem. 6 (2) (1967) 392–394.
[49] R. Jirasko, M. Holcapek, Mass Spec. Rev. 30 (6) (2011) 1013–1036.
[50] P. Tamil Selvi, H. Stoeckli-Evans, M. Palaniandavar, J. Inorg. Biochem. 99 (2005) 2110–2118.